The kinetochore module Okp1[CENP-Q]/Ame1[CENP-U] is a reader for N-terminal modifications on the centromeric histone Cse4[CENP-A]

Ekaterina A Anedchenko[1,†], Anke Samel-Pommerencke[1,†], Tra My Tran Nguyen[1], Sara Shahnejat-Bushehri[1], Juliane Pöpsel[1], Daniel Lauster[2], Andreas Herrmann[2], Juri Rappsilber[3,4] (iD), Alessandro Cuomo[5], Tiziana Bonaldi[5] (iD) & Ann E Ehrenhofer-Murray[1,*] (iD)

Abstract

Kinetochores are supramolecular assemblies that link centromeres to microtubules for sister chromatid segregation in mitosis. For this, the inner kinetochore CCAN/Ctf19 complex binds to centromeric chromatin containing the histone variant CENP-A, but whether the interaction of kinetochore components to centromeric nucleosomes is regulated by posttranslational modifications is unknown. Here, we investigated how methylation of arginine 37 (R37Me) and acetylation of lysine 49 (K49Ac) on the CENP-A homolog Cse4 from *Saccharomyces cerevisiae* regulate molecular interactions at the inner kinetochore. Importantly, we found that the Cse4 N-terminus binds with high affinity to the Ctf19 complex subassembly Okp1/Ame1 (CENP-Q/CENP-U in higher eukaryotes), and that this interaction is inhibited by R37Me and K49Ac modification on Cse4. *In vivo* defects in *cse4-R37A* were suppressed by mutations in *OKP1* and *AME1*, and biochemical analysis of a mutant version of Okp1 showed increased affinity for Cse4. Altogether, our results demonstrate that the Okp1/Ame1 heterodimer is a reader module for posttranslational modifications on Cse4, thereby targeting the yeast CCAN complex to centromeric chromatin.

Introduction

The proper segregation of chromosomes during mitosis is essential for the faithful transmission of genetic information from the mother to the daughter cell, and errors in this process contribute to carcinogenesis and sterility in humans. For segregation, kinetochores are assembled at the centromeres of the chromosomes and provide the contact to the microtubules that pull the sister chromatids apart during mitosis (Musacchio & Desai, 2017). Centromeric chromatin is defined by the presence of the histone H3 variant CENP-A (centromere protein A; Earnshaw & Migeon, 1985), which replaces canonical H3 at centromeric nucleosomes that are interspersed with H3-containing nucleosomes in higher eukaryotes (Bodor *et al*, 2014). The yeast *Saccharomyces cerevisiae* possesses a point centromere with a single nucleosome containing the CENP-A homolog Cse4, around which ~125 bp of centromeric DNA (CEN) are wrapped (Stoler *et al*, 1995; Meluh *et al*, 1998). Cse4 contains a histone fold domain that is homologous to CENP-A in other organisms. In addition, it has an extended N-terminal domain of 135 amino acids that is specific to closely related fungi and is essential for centromere function (Keith *et al*, 1999). The yeast kinetochore serves as a model for kinetochores from higher eukaryotes, which are thought to consist of modular repeats of this kinetochore unit (Westermann & Schleiffer, 2013).

The core kinetochore is a large multiprotein complex consisting of ~30 unique proteins in *S. cerevisiae* (Musacchio & Desai, 2017) that are assembled in modules, several of which are present in multiple copies (Joglekar *et al*, 2009). At the outer kinetochore, the KMN network provides the contact to the microtubule (Fig 1; Varma & Salmon, 2012). Here, several copies of the Ndc80 complex (Wigge & Kilmartin, 2001), which is a dumbbell-shaped structure, interact with the Dam1 ring (Nogales & Ramey, 2009). This ring encircles the microtubule and links the kinetochore to the mitotic spindle. At

1 Department of Molecular Cell Biology, Institut für Biologie, Humboldt-Universität zu Berlin, Berlin, Germany
2 Department of Experimental Biophysics, Institut für Biologie, Humboldt-Universität zu Berlin, Berlin, Germany
3 Wellcome Trust Centre for Cell Biology, School of Biological Sciences, University of Edinburgh, Edinburgh, UK
4 Department of Bioanalytics, Institute of Biotechnology, Technische Universität Berlin, Berlin, Germany
5 Department of Experimental Oncology, European Institute of Oncology, Milan, Italy
   *Corresponding author. Tel: +49 30 2093 49630; E-mail: ann.ehrenhofer-murray@hu-berlin.de
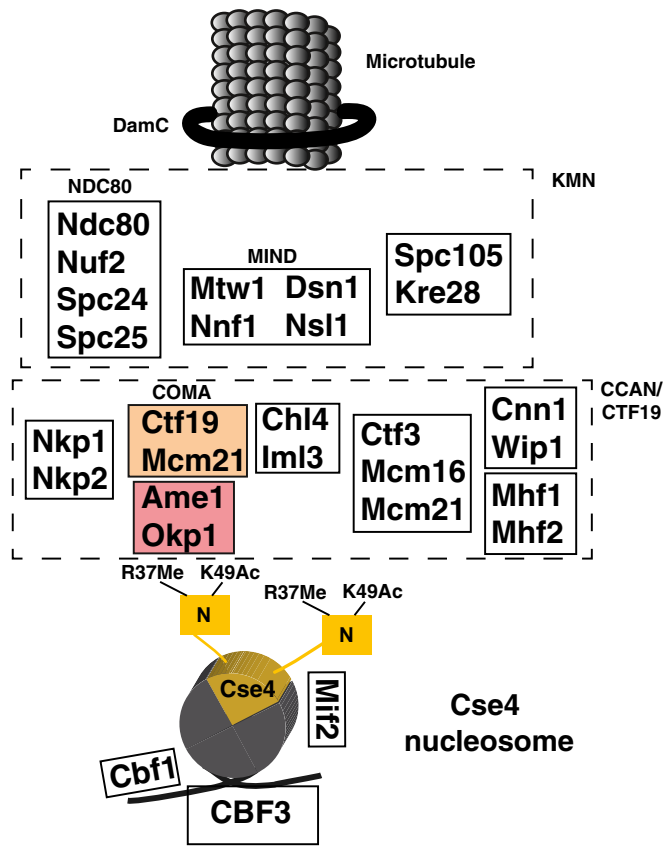   †These authors contributed equally to this work

Figure 1. Overview of proteins of the yeast kinetochore.
The Cse4-containing nucleosome is depicted with the extended N-terminus, which carries R37Me and K49Ac. COMA subunits are shown in colour.

its centromere-proximal side, the Ndc80 complex contacts the MIND complex (Kudalkar *et al*, 2015).

On the chromatin-proximal side of the kinetochore, the Ctf19 complex is an important component of the inner kinetochore that interacts with centromeric chromatin and serves as an assembly platform for the outer kinetochore (Foltz *et al*, 2006; Izuta *et al*, 2006; Okada *et al*, 2006). The Ctf19 complex is the yeast equivalent of the constitutive centromere-associated network (CCAN) in higher eukaryotes and contains 11 other proteins (Hornung *et al*, 2014). The COMA complex represents a subassembly within the Ctf19 complex, and it links the inner kinetochore to the MIND complex (De Wulf *et al*, 2003). COMA was named for the *S. cerevisiae* components Ctf19[CENP-P] (Hyland *et al*, 1999), Okp1[CENP-Q] (Ortiz *et al*, 1999), Mcm21[CENP-O] (Poddar *et al*, 1999) and Ame1[CENP-U] (Burns *et al*, 1994; Cheeseman *et al*, 2002; Gavin *et al*, 2002; superscript indicates the mammalian orthologs). The mammalian equivalent of yeast COMA is the CENP-O/P/Q/U complex (Musacchio & Desai, 2017).

Ctf19 and Mcm21 both contain RWD domains and together form a Y-shaped heterodimer with flexible N-terminal extensions (Schmitzberger & Harrison, 2012). This heterodimer interacts with the Okp1/Ame1 heterodimer via Okp1 residues 317–343 (Schmitzberger *et al*, 2017). Loss of this contact results in the

disruption of binding of two Ctf19 components, Chl4[CENP-N] and Iml3[CENP-L], at the centromere. Next to its binding to Ctf19/Mcm21, Okp1/Ame1 furthermore forms a platform for interactions with other components of the Ctf19 complex, for instance Nkp1/Nkp2, as well as to Mif2[CENP-C], which binds the Cse4-containing nucleosome (Kato *et al*, 2013; Falk *et al*, 2016; Xiao *et al*, 2017). Okp1/Ame1 also connects COMA to the outer kinetochore by interacting with the MIND complex (Hornung *et al*, 2014).

Apart from the interaction with Mif2, little is known about how COMA is recruited to the centromeric nucleosome and how this may be regulated during the cell cycle. Ctf19 was shown to interact by two-hybrid analysis with Cse4 (Ortiz *et al*, 1999), but this has not been confirmed using biochemical methods. Furthermore, Okp1/Ame1 interacts with DNA, but the interaction is not specific to centromeric sequences (Hornung *et al*, 2014). Of note, the genes encoding Okp1, Ame1 and Mif2, but not other components of the Ctf19 complex, are essential for viability, implying that they perform non-redundant functions at the centromere.

One possibility to regulate protein–protein interactions is by post-translational modification (PTM). PTMs on histones are widely used to regulate chromatin function by altering interactions with chromatin-binding proteins ("reader modules"; Patel & Wang, 2013). Such readers include bromo- or YEATS domains for histone acetylation and chromo-, tudor- and PWWP domains for arginine or lysine methylation. However, this type of regulation has not been described for centromeric chromatin, and no reader modules are known within kinetochore proteins.

Next to canonical histone modifications, PTMs have also been discovered in CENP-A homologs. In human cells, serine 7 (S7) in the N-terminus of CENP-A is phosphorylated by Aurora kinase during mitosis (Zeitlin *et al*, 2001; Kunitoku *et al*, 2003), and CENP-A is furthermore phosphorylated at S16 and S18 (Bailey *et al*, 2013). Also, the initiating methionine of CENP-A is cleaved, and the α-amino group of glycine 1 is trimethylated by NRMT1 (Sathyan *et al*, 2017). The absence of this modification reduces the recruitment of CCAN components to the centromere.

Furthermore, several PTMs are known on Cse4 from *S. cerevisiae*. It is ubiquitylated by the ubiquitin ligase Psh1, which controls the levels of Cse4 in the cell and thus restricts its localization to centromeres (Hewawasam *et al*, 2010; Ranjitkar *et al*, 2010). In our earlier work, we identified the methylation of arginine 37 (R37Me), which lies in the essential N-terminal domain (END) of Cse4 (Keith *et al*, 1999), as a modification whose absence causes severe synthetic genetic interactions in combination with deletions or mutations in genes encoding proteins of the COMA subcomplex of the Ctf19 complex, arguing that mutation of this site disturbs the interaction of Cse4 with a kinetochore component (Samel *et al*, 2012). Cse4 is furthermore acetylated on lysine 49 and phosphorylated on S22, S33, S40 and S105 (Boeckmann *et al*, 2013). While Cse4-S33 phosphorylation plays a role in histone deposition at the centromere (Hoffmann *et al*, 2018), the functional role of the other PTMs has not been resolved.

Here, we have investigated the molecular mechanism by which Cse4-R37 methylation and Cse4-K49 acetylation regulate the recruitment of the kinetochore to the centromere. Through genetic screens, we identified mutations in *OKP1* (among others, *okp1-R164C*) and *AME1* (among others, *ame1-273**) that suppress synthetic growth defects of *cse4-R37A*. This suggested a) that Okp1/Ame1 binds the

Cse4 N-terminus, and b) that Okp1/Ame1 binding to mutant Cse4 is restored by the suppressor mutations. In agreement with this, we found Okp1/Ame1 to form a stable complex *in vitro* with the Cse4 N-terminus, whereas no binding to Ctf19/Mcm21 was observed. Importantly, *in vitro* studies using microscale thermophoresis showed that the binding affinity of Cse4 to Okp1/Ame1 was reduced by R37 methylation and K49 acetylation, and this defect in binding to modified Cse4 was suppressed by Okp1-R164C. Altogether, our results demonstrate that Okp1/Ame1 is a reader module for the N-terminus of Cse4. It tethers the kinetochore to centromeric chromatin by binding to Cse4, and this interaction is inhibited by Cse4-R37 methylation and Cse4-K49 acetylation.

Results

Suppression of Cse4-R37 mutation by *okp1-R164C*

Cse4 is methylated on R37 (Fig 2A), and mutation of this site (*cse4-R37A*) causes a synthetic growth defect in cells lacking Cbf1 (*cbf1Δ*; Samel *et al*, 2012). Cbf1 binds the CDEI element of centromeric sequences (Cai & Davis, 1990). Posttranslational modifications on proteins can exert their function by regulating the interaction with another protein. We hypothesized that the growth defect of *cbf1Δ cse4-R37A* is caused by the abrogation of an interaction between Cse4 and an interaction partner, possibly a kinetochore protein. To identify this factor, we isolated mutations that suppress the temperature-sensitive growth defect of *cbf1Δ cse4-R37A*. We surmised that some of these mutations might improve the binding of the hypothesized factor to the mutant N-terminus of Cse4 and therefore restore centromere function. Several mutants were isolated, and the site of the extragenic suppressor was determined by whole-genome sequencing. Interestingly, we obtained one isolate that carried a mutation in *OKP1*, which encodes the COMA component Okp1 (Ortiz *et al*, 1999). The mutation causes the change of arginine 164 of Okp1 to cysteine (*okp1-R164C*), a residue that lies within the "core" region (amino acids 166–211) that is essential for viability (Schmitzberger *et al*, 2017). We constructed the *okp1-R164C* mutation *de novo* and tested its ability to suppress the temperature sensitivity of *cbf1Δ cse4-R37A*. Significantly, while *cbf1Δ cse4-R37A* cells showed a pronounced growth defect at elevated temperatures, this growth defect was suppressed by *okp1-R164C* (Fig 2B). A tentative biochemical interpretation of this genetic suppression is that Okp1 interacts with the N-terminus of Cse4, and that this interaction is regulated by methylation of R37.

We further determined whether other defects of *cse4-R37A* (Samel *et al*, 2012) were also suppressed by *okp1-R164C*. Indeed, *okp1-R164C* also suppressed the growth defect of *cse4-R37A* with mutations/deletions of other Ctf19 complex components (Fig 2C and D, Table 1). There was one notable exception to this, which is that the lethality of *cse4-R37A* with *ame1-4* was not suppressed by *okp1-R164C* (Fig 2D). This observation is interesting in light of the fact that Okp1 and Ame1 are Ctf19 complex components that are essential for viability, and they form a heterodimer *in vitro* (Hornung *et al*, 2014).

cse4-R37A causes defects in chromosome and mini-chromosome segregation at centromeres that are compromised for CDEI function, which can be measured as an increased loss of plasmids that lack

the CDEI sequence (Samel *et al*, 2012). Since *okp1-R164C* suppressed the temperature sensitivity of *cbf1Δ cse4-R37A*, we tested whether it also suppressed the plasmid maintenance defect of *cse4-R37A*. Indeed, while *cse4-R37A* caused an increased loss rate of a plasmid lacking CDEI (CEN ΔCDEI), this defect was decreased by additional *okp1-R164C* mutation (Fig 2E), showing that *okp1-R164C* suppressed the segregation defect of *cse4-R37A* at centromeres lacking CDEI function.

cse4-R37A furthermore causes a cell-cycle arrest at the G2/M phase transition in *cbf1Δ* at the restrictive temperature (Samel *et al*, 2012), which reflects its defect in chromosome segregation. We therefore tested the effect of *okp1-R164C* on cell-cycle progression in *cbf1Δ cse4-R37A* by measuring the DNA content of cells by FACS analysis. Importantly, while *cbf1Δ cse4-R37A* cells showed an accumulation of cells with a 2n DNA content at the restrictive temperature, this arrest was partially suppressed in *cbf1Δ cse4-R37A okp1-R164C* (Fig EV1A), indicating that *okp1-R164C* partially restored centromere function and chromosome segregation to *cse4-R37A*.

We next asked whether other mutations in *OKP1* could be identified that suppressed the defect of *cbf1Δ cse4-R37A*. Through a random mutagenesis of *OKP1*, two strong suppressor alleles, *okp1-E208V* and *okp1-I45T*, and one weaker suppressor, *okp1-S94T,* were isolated (Fig 2F). None of the *okp1* alleles caused a growth defect on their own, nor in the presence of *cbf1Δ* or *cse4-R37A* alone (Fig EV1B–D). Okp1-E208, like R164, lies in the Okp1 core (166–211), the deletion of which is lethal, but is not required for the interaction with Ame1 (Schmitzberger *et al*, 2017), suggesting that it may be an interaction site with Cse4. Okp1-I45 and Okp1-S94 are in the flexible N-terminal region that is dispensable for binding to Ame1 and therefore may also represent a Cse4 binding region. We also tested substitutions of Okp1-R164 to alanine or glutamate, but both were unable to suppress the growth defect of *cbf1Δ cse4-R37A* (Fig EV1E), indicating that the mutation to cysteine bestowed special binding properties upon Okp1. Taken together, this showed that multiple alleles of *OKP1* exist that suppress the defects of *cse4-R37A* and suggested that these alleles restore the hypothesized interaction of Okp1 with the Cse4 N-terminus.

cse4-R37A reduces the recruitment of the MIND complex component Mtw1 to centromeric sequences under restrictive conditions (Samel *et al*, 2012). Since *okp1-R164C* suppressed the growth defect of *cse4-R37A*, we asked whether it also restored binding of Okp1 (Fig 3A) and Ame1 (Fig 3B) to the centromere as measured by chromatin immunoprecipitation (ChIP). Importantly, while the amount of Okp1 and Ame1 associated with *CEN4* was reduced in *cbf1Δ cse4-R37A* cells grown at 37°C, their association was partially restored in *okp1-R164C* cells (Fig 3A and B). Furthermore, *okp1-R164C* restored the association of the MIND component Mtw1 to the centromere (Fig 3C). This indicated that the improved growth of the cells by the *okp1* mutation was achieved by restoring the recruitment of other kinetochore components to the centromeric sequence.

We next asked whether *okp1-R164C* affected the *in vivo* association of Okp1 and Cse4. To test this, co-immunoprecipitation (co-IP) was conducted between Cse4 and Okp1. Wild-type Okp1 was readily co-IPed with wt Cse4 (Fig EV2A). Upon IP of HA-tagged mutant Cse4-R37A, more Okp1-R164C than Okp1 was recovered in the immunoprecipitates (Fig 3D). We observed several bands for Okp1 (the lower bands most likely are proteolytic degradation products of Okp1). Altogether, we conclude that the *in vivo* association between
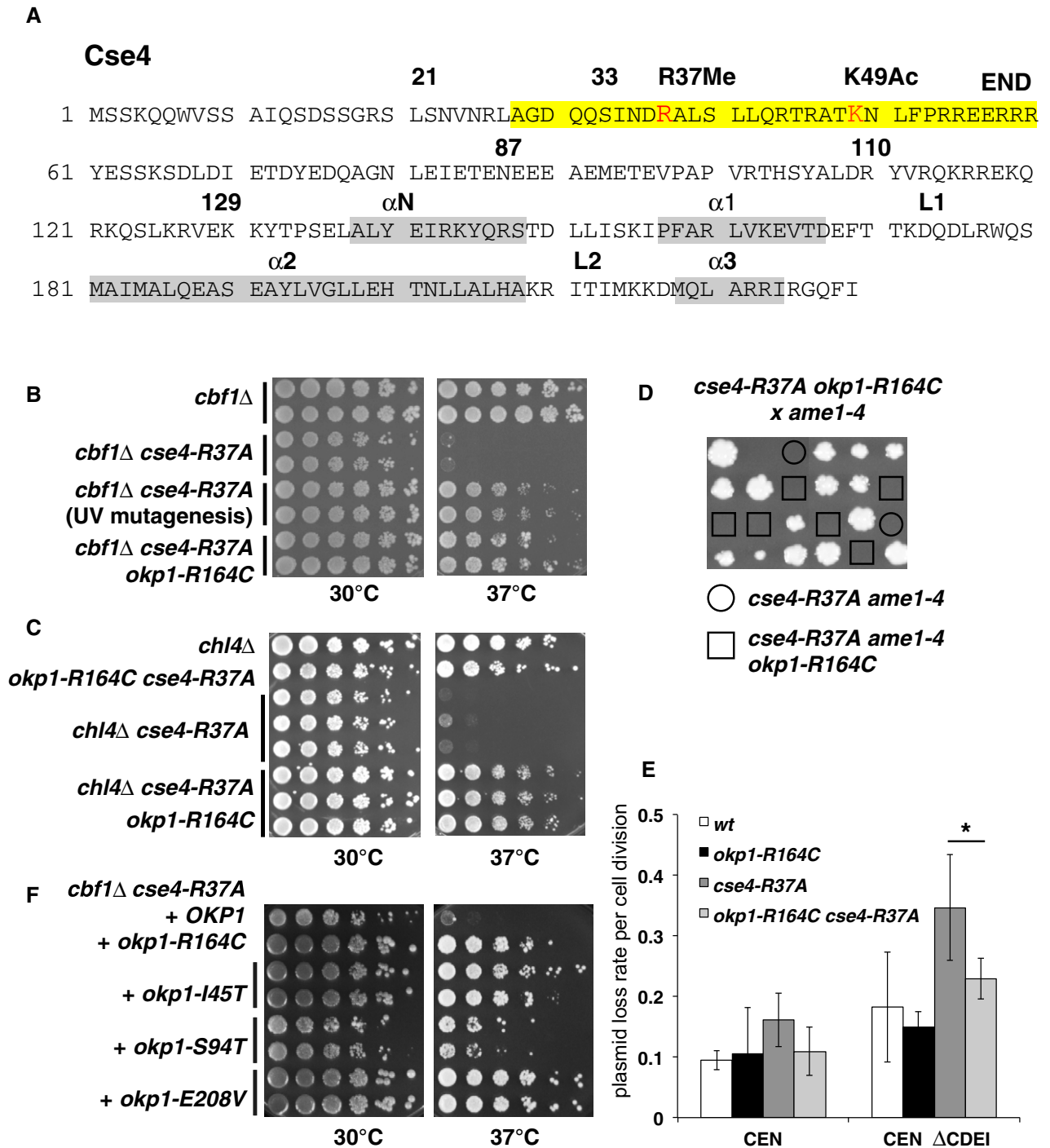
Figure 2. Mutations in *OKP1* suppress growth defects of mutation of Cse4-R37.

A Overview of the amino acid sequence of Cse4. R37Me and K49Ac sites are part of the essential N-terminal domain (END, aa 28–60, yellow) and are indicated in red. The localization of α-helices in the histone fold domain is shown in grey. Amino acid residues that are relevant for this study are indicated with numbers.

B *okp1-R164C* suppressed the temperature-sensitive growth defect of *cbf1Δ cse4-R37A*. Serial dilutions of strains with the indicated genotypes were spotted on full medium and grown for 3 days at 30 or 37°C. The original *okp1-R164C* isolate from the suppressor screen is indicated as "UV mutagenesis".

C *okp1-R164C* suppressed the growth defect of *cse4-R37A* with *chl4Δ*. Representation as in (B).

D *okp1-R164C* was unable to suppress the lethality of *cse4-R37A* with *ame1-4*. Tetrad dissection of a genetic cross between a *cse4-R37A okp1-R164C* and an *ame1-4* strain is shown. The four spores from individual asci are aligned in vertical rows.

E *okp1-R164C* suppressed the maintenance defect of *cse4-R37A* for plasmids lacking the CDEI sequence of CEN6 (CEN ΔCDEI, at 37°C). Error bars give SD of at least three independent transformants. *P = 0.03.

F The *okp1* mutations I45T, S94T and E208V suppressed the temperature-sensitive growth defect of *cbf1Δ cse4-R37A*. Strains with the indicated *okp1* alleles on a plasmid (derivatives of AEY5584) are shown as in (B).

Table 1. Overview of the suppression of *cse4-R37A* phenotypes by *okp1-R164C* and *ame1-273**.

Kinetochore component/complex	Allele	Synthetic phenotype with *cse4-R37A* (Samel *et al*, 2012)	Suppression by *okp1-R164C*	Suppression by by *ame1-273**
Cbf1	*cbf1Δ*	Growth defect	Suppression	Suppression
COMA	*ctf19Δ*	Lethality	Partial suppression	Partial suppression
COMA	*mcm21Δ*	Lethality	Partial suppression	Partial suppression
COMA	*ame1-4*	Lethality	No suppression	n. d.
COMA	*okp1-5*	Growth defect	n.d.	No suppression
Ctf19 complex	*iml3Δ*	Growth defect	Suppression	Suppression
Ctf19 complex	*chl4Δ*	Growth defect	Suppression	Suppression
Ctf19 complex	*ctf3Δ*	Growth defect	Suppression	Suppression

n.d., not determined.

Okp1 and Cse4-R37A (which could be direct or indirect) is improved by *okp1-R164C*.

The Cse4 N-terminus binds Okp1/Ame1

The suppression of *cse4-R37A* defects by mutations in *OKP1* suggests that *cse4-R37A* causes a loss of interaction of the Cse4 N-terminus with Okp1, and that the mutations in Okp1 restore binding of Okp1 to Cse4. We therefore sought to test whether there is a direct interaction between Okp1 and Cse4. To do so, we asked whether a recombinant N-terminal fragment of Cse4 (amino acids 21–129, Cse4N, Fig 2A) interacted *in vitro* with Okp1. Okp1 as obtained by recombinant expression in bacteria was only soluble upon co-expression with Ame1 (Hornung *et al*, 2014), and the two proteins formed a dimer in solution (Okp1/Ame1) as determined by size-exclusion chromatography (SEC, Fig 4A). Importantly, incubation of purified Okp1/Ame1 with recombinant Cse4N yielded a complex that eluted at higher molecular weight by SEC and contained all three proteins (Fig 4A). This demonstrated that Cse4N interacted *in vitro* with Okp1/Ame1, which was in line with our observation of a two-hybrid interaction between Cse4 and Okp1 (Fig EV2B and C).

Since direct contacts between Cse4 and Ctf19 have previously been suggested by two-hybrid analysis (Ortiz *et al*, 1999), we tested whether Cse4N was capable of forming a complex *in vitro* with Ctf19. Recombinant Ctf19 expressed in bacteria was insoluble, but could be obtained in a soluble complex by co-expression with Mcm21 (Schmitzberger & Harrison, 2012; Schmitzberger *et al*, 2017). However, no complex between Cse4N and Ctf19/Mcm21 could be obtained using the same conditions as for Okp1/Ame1 interaction with Cse4N (Fig EV2D). This suggested either that there is no direct interaction, or that the interaction is instable under the conditions used here for SEC. It furthermore indicated that the interaction between the COMA complex and Cse4 is primarily mediated by the Okp1 and Ame1 subunits.

To further query the contacts between the three proteins, we performed chemical cross-linking combined with mass spectrometry (CLMS, Fig 4B, Table EV1; Chen *et al*, 2010). A total of 182 cross-links between the three proteins in the complex formed *in vitro* were mapped, which means that 182 unique residue pairs were identified as being chemically linked, with one residue being in one protein and the other in a different protein. In addition to extensive cross-links between Okp1 and Ame1, we identified several cross-links

between Okp1 and Cse4, thus suggesting a close spatial proximity of the two proteins in the complex formed *in vitro* and accessibility to the cross-linker. Notably, Cse4 lysine 49 (K49) was involved in the formation of seven cross-links to Okp1. Interestingly, the same K49 also showed seven cross-links to Ame1, thus revealing proximity of Cse4 to Ame1 in the *in vitro* complex and suggesting that Cse4N binds in a cleft between Okp1 and Ame1.

Mutations in *AME1* suppress defects of *cse4-R37A*

Next to direct contacts between Cse4N and Okp1, the CLMS analysis above also revealed interactions to Ame1, suggesting that mutations in *AME1* may also be able to suppress the defects of *cse4-R37A*, as is the case for the mutations described above in *OKP1*. To test this, a random mutagenesis of *AME1* was performed in order to isolate suppressor mutations of the temperature-sensitive growth defect of *cbf1Δ cse4-R37A*. Significantly, several alleles were retrieved that caused suppression, namely *ame1-S59P, -N159H, -S275N* and a C-terminal truncation after aa 273 (codon 274 mutated to a stop codon, total length of Ame1 is 324 aa, *ame1-273**, Fig 4C). Residues I273 and S275 are located within segment 1 of Ame1, which interacts with Nkp1/Nkp2, suggesting that abrogation of Nkp1/Nkp2 binding suppresses *cse4-R37A* defects (Schmitzberger *et al*, 2017). Ame1-N159 lies within the Ame1 core, the region that interacts with Okp1, and the mutation therefore may therefore strengthen the interaction to Okp1, or it increases the affinity for Cse4N. Ame1-S59 is in the flexible N-terminal region, but outside of the MIND interaction site at the extreme N-terminus of Ame1.

ame1-273* was furthermore tested for suppression of other *cse4-R37A* phenotypes. Interestingly, suppression was found for all *cse4-R37A* phenotypes, with the exception of the lethality of *cse4-R37A* with *okp1-5* (Table 1), thus revealing a reciprocal relationship between the suppressor alleles in *AME1* and *OKP1*. Furthermore, our ability to isolate *AME1* suppressor alleles was consistent with the existence of a physical interaction between Ame1 and Cse4N as shown by CLMS.

Antagonistic relationship between Cse4-R37 mutation and acetylation on lysine 49

Direct contacts between Cse4N and Okp1/Ame1 involve Cse4 lysine 49. Interestingly, this site is subject to acetylation (K49Ac; Figs 2A
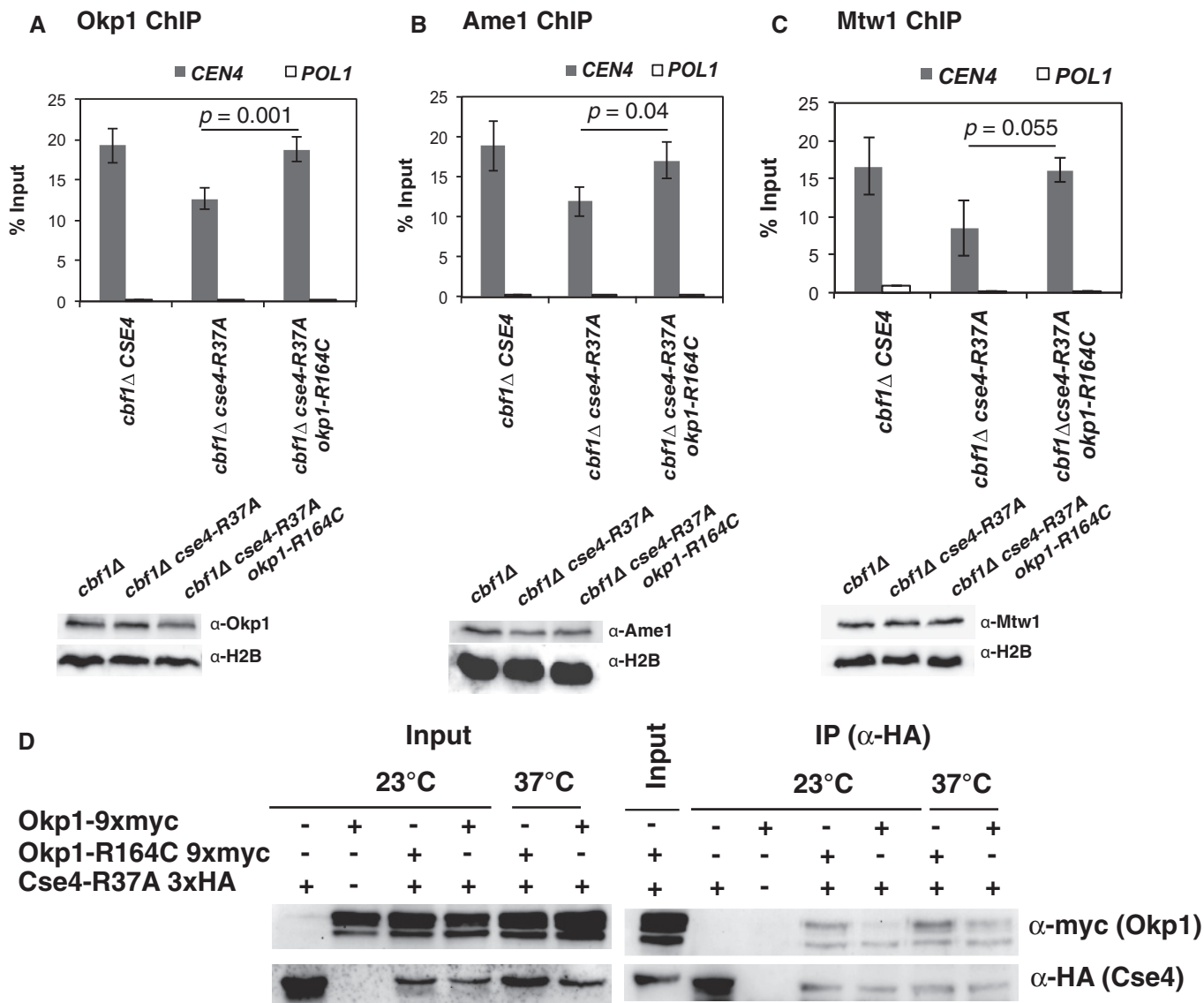
Figure 3. *okp1-R164C* restored binding of kinetochore components to centromeric sequences.

A   *okp1-R164C* restored binding of Okp1 to centromeric sequences. ChIP of 9xmyc-tagged Okp1 was performed in strains with the indicated genotypes that were grown at 37°C for 4 h before ChIP. Enrichment of *CEN4* and *POL1* (as a control) relative to input is given. Below, Western blot analysis of the amounts of 9xmyc-Okp1 and histone H2B (loading control) in whole cell extracts.

B   *okp1-R164C* restored binding of Ame1 to centromeric sequences. ChIP of 9xmyc-tagged Ame1 was performed as in (A). Below, Western blot analysis of the amounts of 9xmyc-Ame1 and H2B as in (A).

C   *okp1-R164C* restored binding of Mtw1 to centromeric sequences. ChIP of 9xmyc-Mtw1 and Western blots (*right*) are presented as in (A) and (B).

D   *okp1-R164C* improved *in vivo* association of Okp1 with Cse4-R37A. Co-immunoprecipitation of Cse4-R37A and Okp1 was carried out in cells carrying *cse4-R37A* with (+) or without (−) 3xHA-tag and *OKP1* or *okp1-R164C* with (+) or without (−) 9xmyc-tag (AEY5040, AEY5972, AEY5973, AEY6589, AEY6592). Cells were grown at 23°C or were shifted to 37°C for 5 h prior to harvesting. Cse4-R37A was immunoprecipitated using an α-HA antibody, and the presence of Cse4-R37A and Okp1 or Okp1-R164C in the immunoprecipitate was tested by Western blotting with α-HA and α-myc antibody, respectively. Left, inputs (the two bands indicate Okp1 and a shorter degradation product); right, α-HA immunoprecipitates.

Data information: (A–C) Mean ± SD, *n* = 4 (*P*-values determined by Student's *t*-test).
Source data are available online for this figure.

and EV3A; Boeckmann *et al*, 2013). Our semi-quantitative analysis showed that 58% of Cse4 from asynchronous cells carried K49Ac (Fig EV3B). To further characterize the modification, we generated an antibody specific for Cse4-K49Ac (Fig EV3C). This antibody recognized wild-type (wt) Cse4 purified from yeast, but not Cse4 in

which K49 was mutated to arginine (K49R; Fig EV3D), and was able to immunoprecipitate Cse4, but not a Cse4 version in which K49 is mutated to arginine (Cse4-K49R; Fig EV4A), further confirming that Cse4 is acetylated on Cse4 *in vivo*. Interestingly, Cse4-K49Ac was enriched in cells arrested in S-phase and G2/M phase as compared
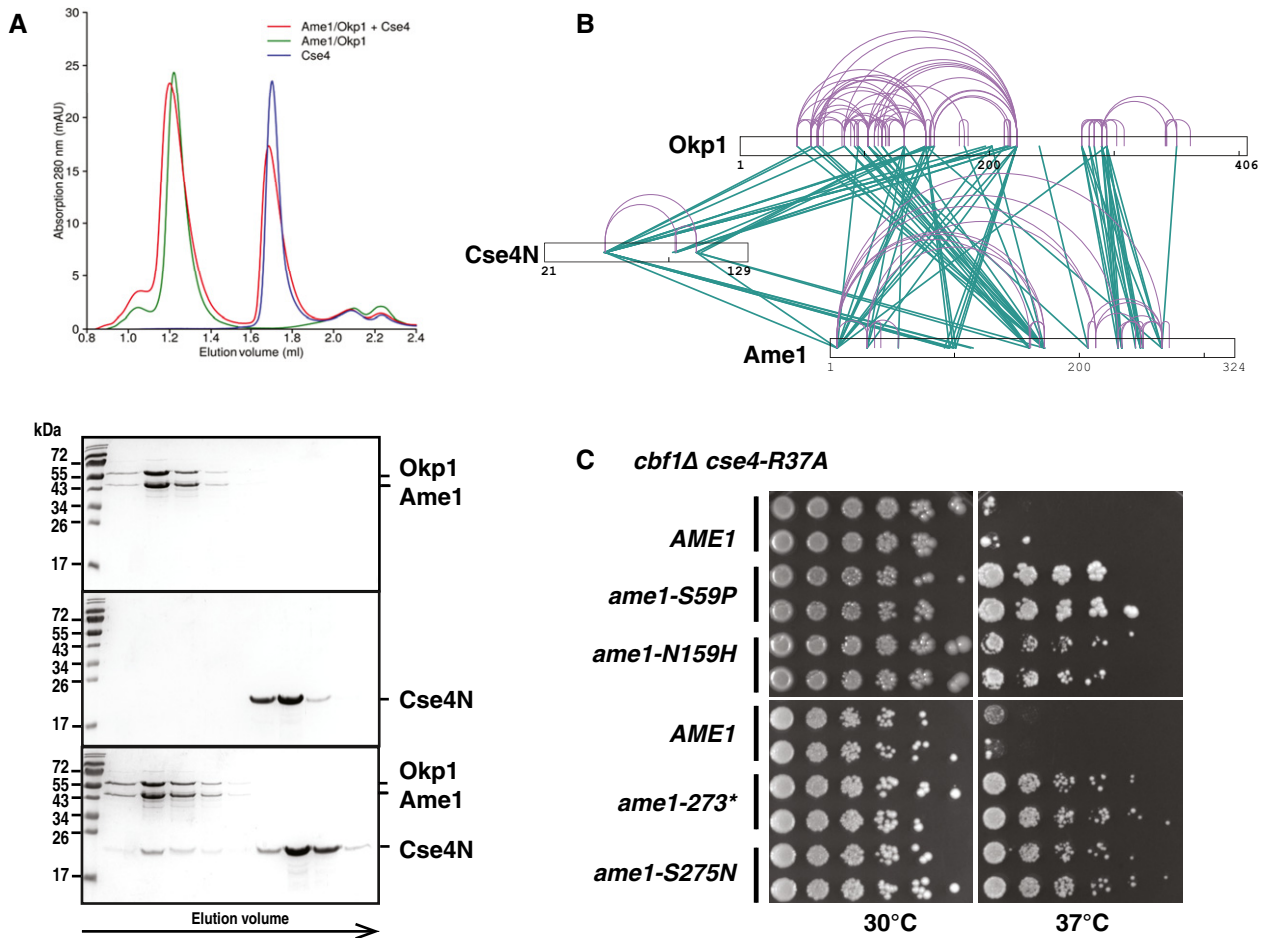
Figure 4. The N-terminus of Cse4 interacts *in vitro* with Okp1/Ame1.

A   Cse4 (21–129, Cse4N) and Okp1/Ame1 were expressed and purified separately from bacteria and co-incubated before separation by analytical gel filtration. Top, representative size-exclusion chromatography (SEC) chromatogram with absorbance measurements at 280 nanometres (nm) is shown. Below, image of Coomassie Blue-stained SDS–PAGE gels with fractions from principal SEC peaks of runs with Okp1/Ame1 alone (top), Cse4N alone (middle) and Okp1/Ame1 preincubated with Cse4N before SEC (bottom). Molecular weight standards are shown in kilodalton (kDa).

B   Intersubunit and self-link map for the Cse4N/Okp1/Ame1 complex formed *in vitro* show direct contacts of Cse4N with both Okp1 and Ame1. Self-links and intersubunit cross-links are coloured in purple and green, respectively.

C   The *ame1* mutations S59P, N159H, S275N and a C-terminal truncation after aa 273 (*ame1-273**) suppressed the growth defect of *cbf1Δ cse4-R37A*. *cbf1Δ cse4-R37A ame1Δ* strains carrying the indicated plasmid-borne *ame1* alleles are shown as in Fig 2B.

Source data are available online for this figure.

to G1-arrested cells (Fig 5A, left), suggesting that Cse4-K49Ac has a regulatory function during the S-phase of the cell cycle. Cse4-R37 methylation was also mildly increased in S-phase (Fig 5A, right), arguing for a potential coordination of the appearance of K49 acetylation and R37 methylation during S-phase.

We next asked how the absence of K49Ac affected Cse4 function. Mutation of K49 to arginine (*cse4-K49R*), which imitates the deacetylated state, did not affect cell viability (Fig 5B), nor did we observe synthetic genetic interactions with deletions or mutations in kinetochore components. Importantly, however, we observed a genetic interaction with *cse4-R37A*. While *cse4-K49R* on its own in *cbf1Δ* did not cause a growth defect, simultaneous mutation of K49R in *cse4-R37A* (*cse4-R37A-K49R*) partially suppressed the growth defect of *cbf1Δ cse4-R37A* (Fig 5B). Furthermore, *cse4-R37A-K49R* suppressed the lethality of *cse4-R37A* with the deletion

of *CTF19*, which encodes a component of the COMA complex (Fig 5C). This suggested that when the interaction of Cse4 with Okp1 is disrupted by *cse4-R37A*, acetylation of K49 has a detrimental effect on Cse4 function. To further test this notion, we tested the effect of mutation of K49 to glutamine (K49Q), which mimics the acetylated state of K49. Interestingly, *cse4-K49Q* was unable to suppress the lethality of *ctf19Δ cse4-R37A* (*cse4-R37A-K49Q*, Fig EV4B), suggesting that the absence of acetylation suppresses the defects of *cse4-R37A*.

One potential explanation for the rescue of *cse4-R37A* phenotypes by *cse4-K49R* is that this is because Cse4-K49R is not degraded during S-phase (Wisniewski *et al*, 2014). However, we observed similar levels of both Cse4 and Cse4-K49R in asynchronous and in S-phase-arrested cells (Fig EV4C), which argued against a role for K49Ac in Cse4 degradation.
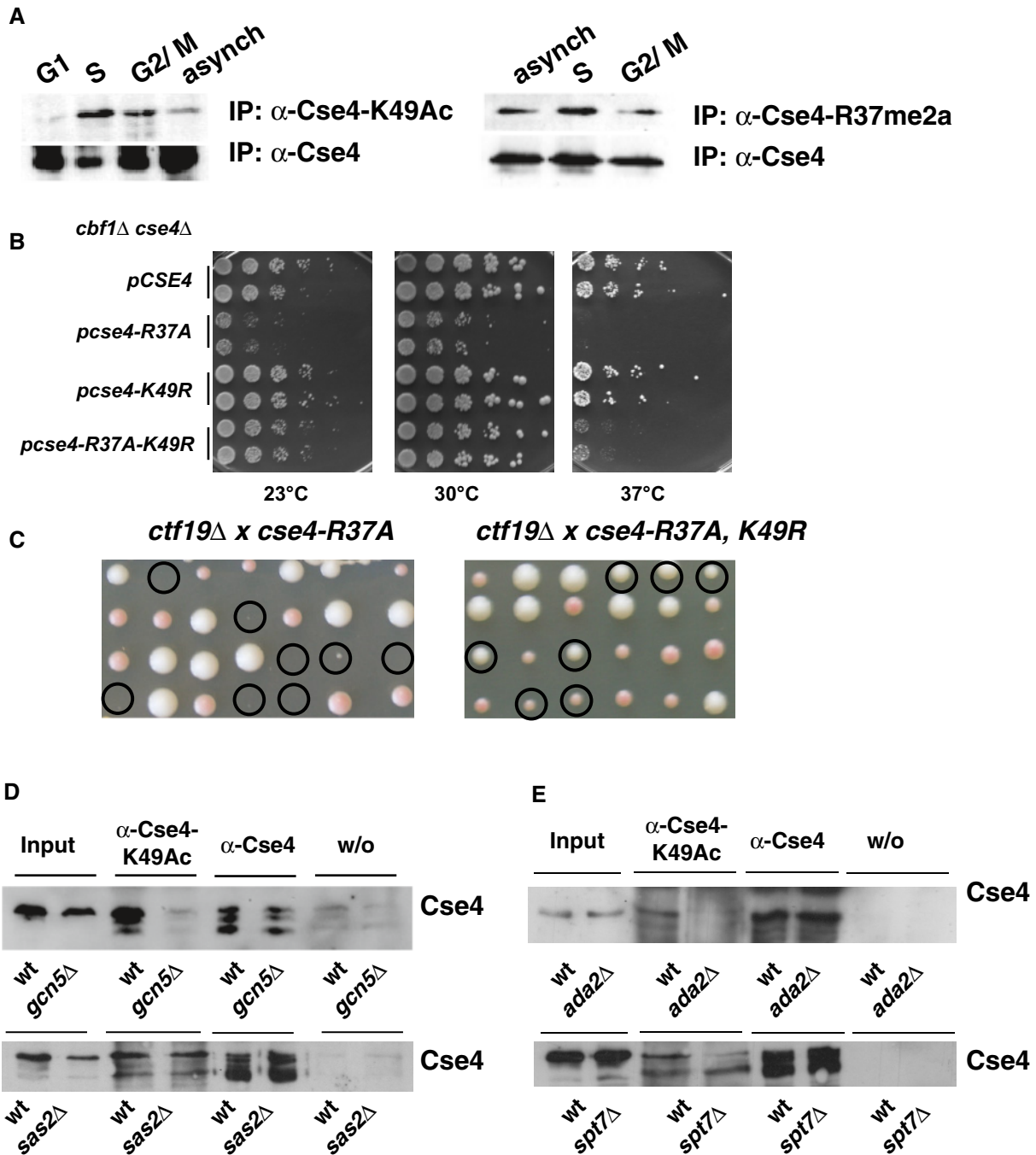
Figure 5. Acetylation of Cse4 K49 counteracts mutation of Cse4-R37.

A   Cse4-K49Ac and –R37Me are increased in S-phase of the cell cycle. Cells carrying 3xHA-tagged Cse4 were used to immunoprecipitate Cse4 with an α-Cse4-K49Ac (left, top) and an α-HA antibody (left, bottom). To detect Cse4-R37 methylation, 3xHA-tagged Cse4 was immunoprecipitated with an α-Cse4-R37me2a (right, top; Samel *et al*, 2012) and an α-HA antibody (right, bottom). Western blots were probed for the presence of Cse4 with the α-HA antibody. G1, treatment with α-factor; S, arrest with hydroxyurea; G2/M, arrest in nocodazole; asynch, asynchronous culture.

B   Mimicking the unacetylated state of Cse4-K49 (*cse4-K49R*) partially suppressed the temperature sensitivity of *cbf1Δ cse4-R37A*. *cbf1Δ cse4Δ* strains carrying the indicated *cse4* alleles on a plasmid were spotted on full medium and grown as in Fig 2B.

C   *cse4-K49R* suppressed the lethality of *cse4-R37A* with *ctf19Δ*. Tetrad dissection of a *ctf19Δ* strain crossed with *cse4-R37A* (left) and *cse4-R37A K49R* (right). Representation as in Fig 2D.

D   Acetylation of Cse4-K49 was reduced in the absence of Gcn5 and the SAGA complex, but not in the absence of the HAT Sas2. Cse4 was precipitated as in (A) from strains wild-type (wt) or *gcn5Δ* (top) or *sas2Δ* strains (bottom) carrying HA-tagged Cse4. w/o, control immunoprecipitation without antibody.

E   Cse4-K49Ac depended on the SAGA components Ada2 and Spt7. Cse4-K49Ac was determined as in (A, left) with cells carrying *ada2Δ* or *spt7Δ*.

Source data are available online for this figure.

Cse4-K49Ac depends on the Gcn5/SAGA histone acetyltransferase complex

The acetylation of histones and non-histone proteins is performed by (histone) acetyltransferase (HAT) complexes (Roth *et al*, 2001), and we next sought to address which of the known HATs/HAT complexes in yeast were responsible for Cse4-K49 acetylation. Importantly, we observed that the absence of the HAT Gcn5 (Brownell *et al*, 1996) abrogated the ability of Cse4 to be immunoprecipitated with the α-Cse4-K49Ac antibody (Fig 5D), thus showing that Gcn5 was responsible for a large part of Cse4-K49Ac. In contrast, no effect was observed in the absence of the HATs Sas2 (Fig 5D; Reifsnyder *et al*, 1996; Ehrenhofer-Murray *et al*, 1997), Sas3 (John *et al*, 2000), Hpa2 (Angus-Hill *et al*, 1999), Hat1 and Elp3 (Wittschieben *et al*, 1999; Fig EV4D and E), indicating that they are not major HATs for Cse4-K49.

Gcn5 is part of three multiprotein complexes, SAGA, ADA and SLIK/SALSA. SAGA is composed of several smaller modules (Daniel & Grant, 2007). Interestingly, the absence of Ada2 and Spt7, components of the SAGA HAT and architecture unit, respectively (Grant *et al*, 1997), abrogated Cse4-K49Ac (Fig 5E). In contrast, the absence of Ubp8, a component of the DUB module (Henry *et al*, 2003), and Ahc1, a component unique to the ADA complex (Eberharter *et al*, 1999), did not affect Cse4-K49Ac (Fig EV4E). Taken together, these results showed that the HAT activity of SAGA/SLIK, but not the deubiquitination activity or the ADA complex, was required for Cse4-K49 acetylation *in vivo*.

Inhibition of Cse4 interaction with Okp1/Ame1 by Cse4-R37 methylation and K49 acetylation

The biochemical analysis above showed that the N-terminal region of Cse4 interacts with Okp1/Ame1. Furthermore, genetic interactions between mutations of Cse4-R37, Cse4-K49 and Okp1 or Ame1

suggested that this interaction is modulated by posttranslational modifications on the Cse4 residues. To investigate this, we sought to determine the binding of Cse4 to Okp1/Ame1 in dependence of R37 and K49 PTMs. Since recombinant Cse4 from *E. coli* is unmodified, we obtained a synthetic Cse4 (aa 33–110) peptide that includes presumed binding regions based on CLMS (Figs 4B and 2A). This peptide bound to Okp1/Ame1 in a pull-down assay as well as by microscale thermophoresis (MST; Figs 6A and EV5, K_D 129 ± 35 nM). Unfortunately, due to the complexity of the amino acid sequence and the length, synthesis of modified versions of Cse4 (33–110) failed. However, a shorter Cse4 (33–87) peptide that includes one possible binding site could be synthesized with R37Me and K49Ac (or both; Fig 2A). Therefore, to test the effect of these modifications, we performed competition assays to measure the replacement of labelled Cse4 (33–110) by unlabelled Cse4 (33–87).

The inhibition constant (K_I) of unmodified Cse4 (33–87) to Okp1/Ame1 was 18.3 ± 1.49 nM. Importantly, R37 methylation decreased the binding by ~13-fold to a K_I of 238.9 ± 24.51 nM (Fig 6B, Table 2). Furthermore, K49Ac reduced binding to Okp1/Ame1 by ~6.7-fold, as shown by a K_I of the K49-acetylated Cse4 (33–87) peptide of 122.4 ± 19.07 nM. A peptide carrying both R37Me and K49Ac showed lower binding than R37Me or K49Ac alone (299.0 ± 50.84 nM, Fig EV5B and C, Table 2). This demonstrated that both R37Me and K49Ac inhibited the binding of Cse4 to Okp1/Ame1. The reduction of binding by K49Ac was consistent with the genetic observation that mutation of Cse4-K49 to imitate the unacetylated state (K49R) suppressed the defect of *cse4-R37A*.

The genetic suppression of the *cse4-R37A* mutation by *okp1-R164C* suggested that the mutant Okp1-R164C version restores centromere function by showing increased binding to Cse4. To test this hypothesis, we determined the affinity of Okp1-R164C/Ame1 to the unmodified and R37Me/K49Ac-modified Cse4 peptides. Significantly, while wild-type Okp1/Ame1 interacted with R37Me-Cse4
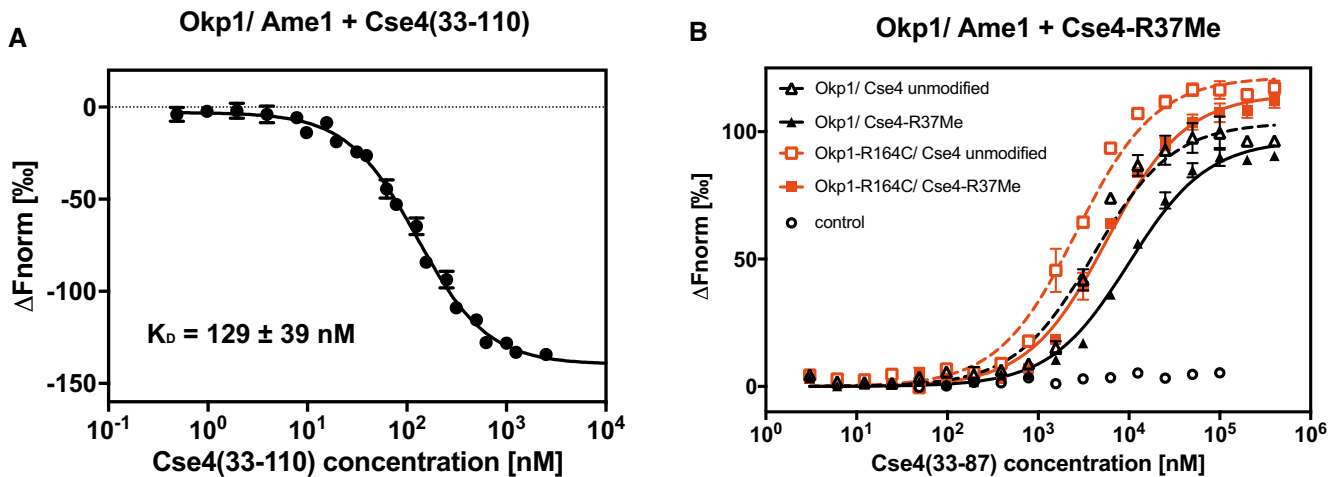
A Okp1/ Ame1 + Cse4(33-110)

K_D = 129 ± 39 nM

B Okp1/ Ame1 + Cse4-R37Me

- △ Okp1/ Cse4 unmodified
- ▲ Okp1/ Cse4-R37Me
- □ Okp1-R164C/ Cse4 unmodified
- ■ Okp1-R164C/ Cse4-R37Me
- ○ control

Figure 6. Methylation of Cse4-R37 and acetylation of Cse4-K49 inhibit binding of Cse4 to Okp1/Ame1.

A   A synthetic 78-aa Cse4 peptide (aa 33–110) binds to Okp1/Ame1 *in vitro*. Microscale thermophoresis (MST) measurement of binding of fluorescently labelled Cse4 (33–110) to Okp1/Ame1 is shown. Normalized fluorescence, from which the fluorescence of unbound Okp1/Ame1 was subtracted (ΔF norm), is plotted against Cse4 (33–110) concentration (logarithmic scale). Mean values ± SD (*n* = 3) are shown.

B   Plot of MST measuring the competition of fluorescently labelled Cse4 (33–110) bound to Okp1/Ame1 (black; or Okp1-R164C/Ame1, red) with unlabelled Cse4 (33–87) that is unmodified or monomethylated on R37 (R37Me). Normalized fluorescence from which the fluorescence of unbound Cse4 (33–110) was subtracted (ΔF norm) is plotted against peptide concentration. Mean values ± standard deviation (*n* = 3) are given. Control, normalized fluorescence of Cse4 (33–110) alone at increasing concentrations.

Table 2. Cse4-R37 methylation and K49 acetylation inhibit the *in vitro* binding of Cse4 to Okp1/Ame1, and binding is restored by Okp1-R164C. Mean ± SD values (*n* = 3) of measurements by microscale thermophoresis as performed in Fig 6 are given.

Peptide	K_I [nM]	
Cse4 (33–87)	Okp1/Ame1	Okp1-R164C/Ame1
Unmodified	18.3 ± 1.49	< 0.1
R37Me	238.9 ± 24.51	68.5 ± 10.67
K49Ac	122.4 ± 19.07	66.3 ± 6.77
R37Me + K49Ac	299.0 ± 50.84	130.1 ± 20.27

peptide with a K_I of 238.9 ± 24.51 nM, Okp1-R164C/Ame1 showed a higher affinity of 68.5 ± 10.67 nM (Fig 6B, Table 2), thus showing that the R164C mutation in Okp1 indeed increased binding of Okp1/Ame1 to the R37-methylated Cse4 N-terminus. R164C also resulted in a higher binding affinity of Okp1/Ame1 to the R37Me + K49Ac as well as the K49Ac Cse4 peptide (Fig EV5B and C, Table 2). Taken together, these results demonstrated that the binding of Cse4 to Okp1/Ame1 is reduced by both R37 methylation and K49 acetylation. Furthermore, the mutation Okp1-R164C improves binding to Cse4, which results in a more efficient recruitment of the Ctf19 complex to the centromeric chromatin *in vivo* and thus in restoration of kinetochore function.

Discussion

Posttranslational modifications on histones regulate gene expression states by modulating the interaction of specific protein domains of chromatin modifiers with the nucleosome (Patel & Wang, 2013). Here, we have identified the Okp1/Ame1 complex from *S. cerevisiae* as a novel reader module for the unmodified N-terminus of the centromeric H3 variant Cse4[CENP-A]. Specifically, Okp1/Ame1 preferentially binds to Cse4, and the binding is inhibited by two modifications, methylation on R37 and acetylation on K49. Hence, Okp1/Ame1 is sensitive to the modification state of Cse4 in the nucleosome and thus regulates the assembly of the kinetochore on centromeric chromatin. We suggest that this regulates the dynamic association of kinetochores to chromatin during the cell cycle.

The discovery of a reader module in the inner kinetochore is unexpected in several ways. Firstly, Okp1/Ame1 contains no sequence motifs that are related to known chromatin readers, such that its identity as a reader of PTMs was unanticipated. Okp1/Ame1 was previously shown to bind DNA *in vitro*, but the *in vivo* relevance of this observation was unknown (Hornung *et al*, 2014). Our results provide clear evidence for a dominant role of Okp1/Ame1 in recognizing centromeric chromatin via the Cse4 N-terminus, thereby linking this to the recruitment of the Ctf19 complex and the hierarchical assembly of the kinetochore.

Secondly, the effect of Cse4 PTMs on Okp1/Ame1 binding is an ~7–13-fold reduction in affinity, which may seem like a relatively subtle change, but this change clearly is sufficient *in vivo* to disrupt binding. Accordingly, the restoration of *in vitro* binding by Okp1-R164C is ~2–4-fold, and again, this seemingly moderate change of *in vitro* binding is sufficient to strongly suppress growth defects

in vivo. We note that the affinity constants measured here were determined with a short (55 aa) Cse4 peptide and lie in the micromolar range, which is a binding strength comparable to that of other PTM readers like the bromodomain of the transcriptional co-activator P/CAF (Dhalluin *et al*, 1999), or tudor domains to methyl-lysine (Lu & Wang, 2013). As expected, the binding of a longer (78 aa) Cse4 peptide to Okp1/Ame1 is stronger (~130 nM), and the full Cse4N (aa 21–121) interacts with low nanomolar affinity. This robust binding of Okp1/Ame1 to Cse4 as a critical contact point at the base of the kinetochore ensures that the contact can resist the strong pulling forces that are exerted on the single Cse4 nucleosome during chromosome segregation.

Thirdly, based on earlier observations, the Cse4 N-terminus was expected to interact with Ctf19/Mcm21 (Ortiz *et al*, 1999), but we were unable to detect such an interaction with purified components. Rather, we identified a tight association to Okp1/Ame1. Our results thus demonstrate that the predominant contact of COMA to chromatin occurs via Okp1/Ame1. This is consistent with the fact that Cse4N, Okp1 and Ame1, but not Ctf19, Mcm21 or other Ctf19 components, are essential for viability.

What is the function of the two PTMs in the Cse4 N-terminus? Yeast kinetochores are associated with centromeric sequences throughout most of the cell cycle, except for a brief period within S-phase where they are released as the centromeric DNA is replicated (Kitamura *et al*, 2007). Also, Cse4 is replaced in early S-phase at the time of DNA synthesis (Wisniewski *et al*, 2014). We speculate that the R37 methylation and K49 acetylation in Cse4N mediate this process by impairing the interaction of COMA to the Cse4-containing nucleosome. In agreement with this notion, K49Ac and R37Me are increased in cells arrested in S-phase. How the respective modifying enzymes (Gcn5/SAGA for K49Ac and an unknown arginine methyltransferase for R37) access their target sites in this context, and whether this is coupled to the deposition of new Cse4, remains to be determined.

With respect to cell-cycle dynamics, it is interesting to note that there has been some debate regarding the exact stoichiometry of Cse4 within the centromeric nucleosome across the cell cycle, or whether it constitutes a hemisome (Henikoff & Furuyama, 2012). The Cse4 content has been proposed to oscillate during mitosis from one to two molecules per centromeric nucleosome (Shivaraju *et al*, 2012), whereas another study observed replacement of Cse4 during S-phase, and it remained stably present at the centromere for the rest of the cell cycle until the next S-phase (Wisniewski *et al*, 2014). If two Cse4 molecules are in the nucleosome, presumably two Okp1/Ame1 entities are bound, raising the question of the stoichiometry of other Ctf19 components relative to Okp1/Ame1. Of note, Okp1 and Ame1 are more abundant in the nucleus than Ctf19 and Mcm21 (Dhatchinamoorthy *et al*, 2017), arguing that not all cellular Okp1/Ame1 is part of COMA. Thus, further work is required to elucidate the precise architecture of the kinetochore at its interface with chromatin.

Our discovery of an Okp1/Ame1 axis for kinetochore recruitment by interaction with Cse4 raises the question how it translates to higher eukaryotic systems, since the Cse4 N-terminus is specific to yeasts (Boeckmann *et al*, 2013) and is not homologous to the N-terminus of CENP-A, e.g. from humans. It will therefore be interesting to determine how CENP-Q/CENP-U makes contacts at its centromere-proximal side, and whether this likewise is regulated by

modifications on that protein. On the other hand, a yeast-specific Okp1/Ame1 recruitment mechanism may extend to pathological yeasts like *Candida albicans*, which shares with *S. cerevisiae* an extended N-terminus on Cse4. Our observations therefore afford a possibility to design molecules that specifically disrupt this interaction and inhibit chromosome segregation and cell growth selectively in yeasts, but not in the human host. Such molecules provide a therapeutic opportunity for the treatment of yeast pathogens.

Materials and Methods

Saccharomyces cerevisiae strains and yeast methods

Yeast strains and plasmids used in this study are described in Tables EV2 and EV3. Yeasts were grown and manipulated using standard genetic techniques (Sherman, 1991). Plasmid-borne alleles of *cse4*, *okp1* and *ame1* were constructed using the gap repair method and verified by sequence analysis. For chromosomal integration of *cse4* and *okp1* alleles, the respective allele was transferred into a *URA3*-marked integrating vector and introduced into the corresponding strain by integrative transformation followed by loop-out on 5-fluoroorotic acid (5-FOA) medium (Boeke *et al*, 1984). For genetic crosses, *cse4* and *okp1* were marked with *HISMX* or *URAMX* by integration of the respective resistance cassettes downstream of the open reading frame. Deletions of chromosomal genes were performed using the integration of knockout cassettes (Longtine *et al*, 1998).

UV mutagenesis of *cbf1Δ cse4-R37A* cells (AEY4984), isolation of suppressor mutants of the temperature sensitivity and identification of the causative mutation were carried out as described (Samel *et al*, 2017). Briefly, DNA of a temperature-resistant derivative (AEY5438) was subjected to whole-genome sequencing, and single-nucleotide polymorphisms were identified by comparing the sequence to that of AEY4984. AEY5438 carried the mutation *okp1-R164C* as well as non-synonymous mutations in two other genes. To determine whether *okp1-R164C* caused the suppression phenotype, the mutation was created by site-directed mutagenesis in an integrative *URA3*-marked plasmid and introduced into AEY4984 by integrative transformation and loop-out as described above. *cbf1Δ cse4-R37A okp1-R164C* strains were identified by sequence analysis of the *okp1* gene and tested for temperature resistance by growth assays on full medium at elevated temperatures.

Plasmid loss was measured in a wt (AEY1), *cse4-R37A* (AEY5596), *okp1-R164C* (AEY5594) and *okp1-R164C cse4-R37A* (AEY5586) strain carrying a CEN6-TRP1 plasmid containing either a functional centromere sequence (pAE264) or a centromere sequence without CDEI element (CENΔCDEI, pAE1771) as previously described (McNally & Rine, 1991).

For FACS analysis, strains were grown in YPD at 23°C and shifted for 5 h to 37°C. Samples of 0.2 OD were harvested in mid-exponential phase at both temperatures. After washing the samples with ddH$_2$O, cells were resuspended in 400 µl ddH$_2$O, sonicated briefly and fixed with 950 µl 100% EtOH at −20°C. For FACS analysis, the cells were washed with 800 µl of 50 mM sodium citrate (pH 7.2) and incubated with 500 µl RNase A solution [0.25 mg/ml in 50 mM sodium citrate (pH 7.2)] overnight at 37°C. The cells were subsequently incubated with 20 µl of 20 mg/ml proteinase K for 2 h at 49°C, sonicated briefly and stained with 500 µl Sytox Green

solution [4 µM Sytox Green in 50 mM sodium citrate (pH 5.2)]. FACS analysis was performed with a BD Accuri flow cytometer.

Screen for suppressor alleles of *OKP1* and *AME1*

Plasmid-borne *OKP1* (pAE2134) was mutagenized by error-prone PCR and introduced by gap repair into a *cbf1Δ cse4-R37A okp1Δ* strain that carried *OKP1* on a *URA3*-marked plasmid (AEY5584). Transformants were plated at the restrictive temperature, and temperature-resistant candidates were isolated. The *URA3*-marked plasmid with wild-type *OKP1* was subsequently eliminated on 5-FOA medium and the temperature resistance verified. For mutagenesis of *AME1*, plasmid-borne *AME1* (pAE2456) was mutagenized by error-prone PCR and introduced into the *cbf1Δ cse4-R37A* strain AEY4984 as above. Mutant *okp1* or *ame1* plasmids, respectively, were isolated, amplified in *E. coli* and subjected to sequence analysis. Plasmids from temperature-resistant *ame1* isolates were further phenotypically tested in a *cbf1Δ cse4-R37A ame1Δ* strain (AEY6091) after counter-selection of the p*URA3-AME1* plasmid on 5-FOA medium. For plasmid isolates that carried several mutations, the causative mutation was identified by constructing plasmids carrying a single mutation by site-directed mutagenesis and testing its ability to suppress the temperature sensitivity of the *cbf1Δ cse4-R37A okp1Δ* or *ame1Δ* strain by plasmid shuffle as described above.

Molecular cloning

The open reading frames corresponding to the Cse4 (21–129), Ctf19 and Mcm21 proteins were amplified from genomic DNA or cDNA (in the case of Mcm21). *CSE4* was cloned into expression vector pETM11 using NcoI/SalI, *CTF19* and *MCM21* were subcloned from the monocistronic pET3aTr vector into the polycistronic expression vector pST39 (cassettes 3 (SacI/KpnI) and 4 (BspEI/MluI), respectively; Tan *et al*, 2005). The pST39/Okp1-R164C-Ame1 construct was obtained based on pST39/Okp1-Ame1 by site-directed mutagenesis using primers GATCCATCTTTGTTTATTAGAGACTAACACTG TAAGC and AGTCTCTAATAAACAAAGTAGGATCCTATCATTATT TT. Constructs were verified by DNA sequencing. The vectors pST39 and pET3aTr were kindly provided by Song Tan (The Pennsylvania State University, USA).

For construction of pAE2123 (= pRS426-*OKP1*), an *OKP1* fragment with 372 basepairs (bp) upstream and 485 bp downstream of the open reading frame (ORF) was PCR-amplified from genomic DNA and cloned with SalI/SacI in pRS426 (Sikorski & Hieter, 1989). To generate pAE2455 (= pRS426-*AME1*), a PCR-amplified *AME1* fragment including 324 bp upstream and 321 bp downstream of ORF was cloned with NotI/SalI into pRS426.

Recombinant protein expression and purification

Plasmids containing the genes of interest were transformed into the *E. coli* strain Rosetta. Cells containing plasmids with Cse4N were grown in auto-induction media to an optical density at 600 nm (OD600) of 0.3 at 37°C and incubated for 24 h at 18°C (Studier, 2005). Ctf19-Mcm21 complex was expressed at 18°C overnight after induction at an OD600 of 0.6 with 0.5 mM IPTG.

For Cse4 (21–129) purification, cells pellet was resuspended in 50 mM Tris–HCl, pH 8.0, 500 mM NaCl, 10 mM imidazole, 0.01%

Tween-20, 1 mM β-mercaptoethanol, 1 mM PMSF, protease inhibitors. Bacteria were lysed by sonication, and protein was isolated using Ni-NTA agarose beads (Qiagen). Washing of beads was performed in 50 mM Tris–HCl, pH 8.0, 300 mM NaCl, 20 mM imidazole, 1 mM β-mercaptoethanol. Cse4 (21–129) was eluted from Ni-NTA beads with 50 mM Tris–HCl, pH 8.0, 300 mM NaCl, 250 mM imidazole, 1 mM β-mercaptoethanol. Fractions containing Cse4 (21–129) were pooled, supplemented with TEV protease and dialysed against 50 mM Tris–HCl, pH 8.0, 300 mM NaCl, 1 mM β-mercaptoethanol at 4°C overnight. Cse4 (21–129) protein without 6× HisTag and TEV protease were separated using Ni-NTA beads. Fractions containing Cse4 (21–129) were concentrated and further separated via Superdex 75 size-exclusion column (GE Healthcare) in 30 mM Tris–HCl, pH 8.0, 300 mM NaCl, 1 mM DTT. Peak fractions were pooled, concentrated and stored at −80°C.

Ame1/Okp1 complex purification was performed as described (Hornung *et al*, 2014) using plasmid pST39 carrying *OKP1* and *AME1* (kindly provided by S. Westermann, University of Duisburg-Essen, Germany).

For Ctf19/Mcm21 complex purification, cells were lysed by sonication in 50 mM HEPES, pH 7.5, 500 mM NaCl, 10% glycerol, 10 mM imidazole, 1 mM β-mercaptoethanol, protease inhibitors. The lysate was incubated with Ni-NTA beads, and bound protein complex was washed and eluted with 50 mM HEPES, pH 7.5, 300 mM NaCl, 10% glycerol, 250 mM imidazole, 1 mM β-mercaptoethanol. The protein solution was diluted to 100 mM NaCl and applied to a MonoQ anion exchange column (GE Healthcare) in 50 mM HEPES, pH 7.5, 100 mM NaCl, 10% glycerol and 1 mM β-mercaptoethanol and eluted with a gradient of 100 mM–1 M NaCl. Pooled fractions were concentrated and further purified on a Superdex 200 size-exclusion column (GE Healthcare) in 30 mM HEPES, pH 7.5, 300 mM NaCl, 10% glycerol, 1 mM DTT. Peak fractions were pooled, concentrated and stored at −80°C.

Interaction studies using SEC

Analytical gel filtration was performed on a Superdex 200 Increase 3.2/300 column under isocratic conditions at 4°C. Proteins were mixed in equimolar ratio in binding buffer (50 mM HEPES, pH 7.5, 200 mM NaCl, 1 mM DTT) and incubated for 20 min on ice. Elution of proteins was monitored by absorbance at a wavelength of 280 nm. The eluates were fractionated, loaded onto SDS–PAGE, and the gels were stained with Coomassie Blue.

Microscale thermophoresis

Measurements were performed using a Monolith NT.115 instrument in Premium coated glass capillaries (Nanotemper). Okp1/Ame1 or Okp1-R164C/Ame1 (starting at 2 μM) was titrated against of 150 nM of labelled Cse4 peptide (33–110) in MST buffer (50 mM HEPES, pH 7.5, 200 mM NaCl, 1 mg/ml BSA and 0.05% Tween-20). The Cse4 (33–110) peptide (Table EV4, 50 μM, CASLO, Kongens Lyngby, Denmark) was labelled with Alexa 647-NHS (600 μM) in the dark overnight at 4°C. Unbound Alexa 647 was removed with a G25 column (GE Healthcare). The labelling of peptide yielded a dye to peptide ratio of 3:1. Okp1/Ame1 or Okp1-R164C/Ame1 complex was incubated with Cse4 (33–110) peptide at RT for 10 min in dark. Then, the mixture was loaded into glass capillaries and measured at

25°C for initial fluorescence and change in fluorescence upon a thermophoresis measurement (setup: MST power: 40%, red LED power: 40%). For analysis, the T-jump with thermophoresis (for 21 s) was used. In order to determine the noise level, triplicates of the same dilution of labelled peptide and protein complex were measured leading to $\Delta F \approx$ FU. The change in fluorescence was expressed as fraction bound of the maximum fluorescence in the bound state. Dissociation constants were deduced from a binding saturation fit of mean values of independent experiments ($n = 3$). The function for fitting (Equation 1) is derived from the law of mass action,

$$F = \frac{1}{2B}\left(B + L + Kd_{app} - \sqrt[2]{\left(B + L + Kd_{app}\right)^2 - 4B*L}\right), \quad (1)$$

with L being the concentration of labelled peptide, B being the concentration of protein with constant concentration and Kd_{app} being the apparent dissociation constant. Data were analysed using Affinity Analysis Software (Nanotemper, v2.0) and plotted with Graphpad Prism 5.

For competition assays, a complex between Ame1/Okp1 dimer (4 μM) and labelled Cse4 peptide (600 nM) was assembled in MST buffer at RT for 10 min in dark. Then, shorter Cse4 (33–87) peptide versions (initial concentration is 800 μM) were titrated against of Okp1-Ame1/Cse4 (33–110) peptide complex in order to replace labelled peptide (Table EV4). Mixtures were loaded on glass capillaries and measured at 25°C for initial fluorescence and change in fluorescence with the thermophoresis measurement (MST power 40% and LED power 40%). Results from competition experiments were analysed according to the same formula (Equation 1); however, the half maximum saturation point was described by a half maximum inhibition value (IC_{50}). In order to convert IC_{50} values into inhibitor constants (K_I), Equation 2 was implemented, which is based on (Nikolovska-Coleska *et al*, 2004) and can be computed with an online tool (http://sw16.im.med.umich.edu/software/calc_ki/).

$$K_i = \frac{[I]_{50}}{\left(\frac{[L]_{50}}{K_d} + \frac{[P]_0}{K_d} + 1\right)} \quad (2)$$

With $[I]_{50}$ being the concentration of free inhibitor at 50% inhibition, $[L]_{50}$ being the concentration of free labelled peptide and $[P]_0$ being the concentration of the free protein at 0% inhibition.

Data availability

- The mass spectrometry data from CLMS of Okp1/Ame1/Cse4N have been deposited to the ProteomeXchange Consortium database (dataset identifier PXD009648).
- For further experimental details and Materials and Methods, please consult the Appendix.

Expanded View for this article is available online.

Acknowledgements

Author contributions

Conflict of interest

References

Angus-Hill ML, Dutnall RN, Tafrov ST, Sternglanz R, Ramakrishnan V (1999) Crystal structure of the histone acetyltransferase Hpa2: a tetrameric member of the Gcn5-related N-acetyltransferase superfamily. *J Mol Biol* 294: 1311–1325

Bailey AO, Panchenko T, Sathyan KM, Petkowski JJ, Pai PJ, Bai DL, Russell DH, Macara IG, Shabanowitz J, Hunt DF, Black BE, Foltz DR (2013) Posttranslational modification of CENP-A influences the conformation of centromeric chromatin. *Proc Natl Acad Sci USA* 110: 11827–11832

Bodor DL, Mata JF, Sergeev M, David AF, Salimian KJ, Panchenko T, Cleveland DW, Black BE, Shah JV, Jansen LE (2014) The quantitative architecture of centromeric chromatin. *Elife* 3: e02137

Boeckmann L, Takahashi Y, Au WC, Mishra PK, Choy JS, Dawson AR, Szeto MY, Waybright TJ, Heger C, McAndrew C, Goldsmith PK, Veenstra TD, Baker RE, Basrai MA (2013) Phosphorylation of centromeric histone H3 variant regulates chromosome segregation in *Saccharomyces cerevisiae*. *Mol Biol Cell* 24: 2034–2044

Boeke JD, LaCroute F, Fink GR (1984) A positive selection for mutants lacking orotidine-5′-phosphate decarboxylase activity in yeast: 5-fluoro-orotic acid resistance. *Mol Gen Genet* 197: 345–346

Brownell JE, Zhou J, Ranalli T, Kobayashi R, Edmondson DG, Roth SY, Allis CD (1996) Tetrahymena histone acetyltransferase A: a homolog to yeast Gcn5p linking histone acetylation to gene activation. *Cell* 84: 843–851

Burns N, Grimwade B, Ross-Macdonald PB, Choi EY, Finberg K, Roeder GS, Snyder M (1994) Large-scale analysis of gene expression, protein localization, and gene disruption in *Saccharomyces cerevisiae*. *Genes Dev* 8: 1087–1105

Cai M, Davis RW (1990) Yeast centromere binding protein CBF1, of the helix-loop-helix protein family, is required for chromosome stability and methionine prototrophy. *Cell* 61: 437–446

Cheeseman IM, Anderson S, Jwa M, Green EM, Kang J, Yates JR III, Chan CS, Drubin DG, Barnes G (2002) Phospho-regulation of kinetochore-microtubule attachments by the Aurora kinase Ipl1p. *Cell* 111: 163–172

Chen ZA, Jawhari A, Fischer L, Buchen C, Tahir S, Kamenski T, Rasmussen M, Lariviere L, Bukowski-Wills JC, Nilges M, Cramer P, Rappsilber J (2010) Architecture of the RNA polymerase II-TFIIF complex revealed by cross-linking and mass spectrometry. *EMBO J* 29: 717–726

Daniel JA, Grant PA (2007) Multi-tasking on chromatin with the SAGA coactivator complexes. *Mutat Res* 618: 135–148

De Wulf P, McAinsh AD, Sorger PK (2003) Hierarchical assembly of the budding yeast kinetochore from multiple subcomplexes. *Genes Dev* 17: 2902–2921

Dhalluin C, Carlson JE, Zeng L, He C, Aggarwal AK, Zhou MM (1999) Structure and ligand of a histone acetyltransferase bromodomain. *Nature* 399: 491–496

Dhatchinamoorthy K, Shivaraju M, Lange JJ, Rubinstein B, Unruh JR, Slaughter BD, Gerton JL (2017) Structural plasticity of the living kinetochore. *J Cell Biol* 216: 3551–3570

Earnshaw WC, Migeon BR (1985) Three related centromere proteins are absent from the inactive centromere of a stable isodicentric chromosome. *Chromosoma* 92: 290–296

Eberharter A, Sterner DE, Schieltz D, Hassan A, Yates JR III, Berger SL, Workman JL (1999) The ADA complex is a distinct histone acetyltransferase complex in *Saccharomyces cerevisiae*. *Mol Cell Biol* 19: 6621–6631

Ehrenhofer-Murray AE, Rivier D, Rine J (1997) The role of Sas2, an acetyltransferase homolog of *Saccharomyces cerevisiae*, in silencing and ORC function. *Genetics* 145: 923–934

Falk SJ, Lee J, Sekulic N, Sennett MA, Lee TH, Black BE (2016) CENP-C directs a structural transition of CENP-A nucleosomes mainly through sliding of DNA gyres. *Nat Struct Mol Biol* 23: 204–208

Foltz DR, Jansen LE, Black BE, Bailey AO, Yates JR III, Cleveland DW (2006) The human CENP-A centromeric nucleosome-associated complex. *Nat Cell Biol* 8: 458–469

Gavin AC, Bosche M, Krause R, Grandi P, Marzioch M, Bauer A, Schultz J, Rick JM, Michon AM, Cruciat CM, Remor M, Hofert C, Schelder M, Brajenovic M, Ruffner H, Merino A, Klein K, Hudak M, Dickson D, Rudi T et al (2002) Functional organization of the yeast proteome by systematic analysis of protein complexes. *Nature* 415: 141–147

Grant PA, Duggan L, Cote J, Roberts SM, Brownell JE, Candau R, Ohba R, Owen-Hughes T, Allis CD, Winston F, Berger SL, Workman JL (1997) Yeast Gcn5 functions in two multisubunit complexes to acetylate nucleosomal histones: characterization of an Ada complex and the SAGA (Spt/Ada) complex. *Genes Dev* 11: 1640–1650

Henikoff S, Furuyama T (2012) The unconventional structure of centromeric nucleosomes. *Chromosoma* 121: 341–352

Henry KW, Wyce A, Lo WS, Duggan LJ, Emre NC, Kao CF, Pillus L, Shilatifard A, Osley MA, Berger SL (2003) Transcriptional activation via sequential histone H2B ubiquitylation and deubiquitylation, mediated by SAGA-associated Ubp8. *Genes Dev* 17: 2648–2663

Hewawasam G, Shivaraju M, Mattingly M, Venkatesh S, Martin-Brown S, Florens L, Workman JL, Gerton JL (2010) Psh1 is an E3 ubiquitin ligase that targets the centromeric histone variant Cse4. *Mol Cell* 40: 444–454

Hoffmann G, Samel-Pommerencke A, Weber J, Cuomo A, Bonaldi T, Ehrenhofer-Murray AE (2018) A role for CENP-A/Cse4 phosphorylation on serine 33 in deposition at the centromere. *FEMS Yeast Res* 18: fox094

Hornung P, Troc P, Malvezzi F, Maier M, Demianova Z, Zimniak T, Litos G, Lampert F, Schleiffer A, Brunner M, Mechtler K, Herzog F, Marlovits TC, Westermann S (2014) A cooperative mechanism drives budding yeast kinetochore assembly downstream of CENP-A. *J Cell Biol* 206: 509–524

Hyland KM, Kingsbury J, Koshland D, Hieter P (1999) Ctf19p: a novel kinetochore protein in *Saccharomyces cerevisiae* and a potential link between the kinetochore and mitotic spindle. *J Cell Biol* 145: 15–28

Izuta H, Ikeno M, Suzuki N, Tomonaga T, Nozaki N, Obuse C, Kisu Y, Goshima N, Nomura F, Nomura N, Yoda K (2006) Comprehensive analysis of the ICEN (Interphase Centromere Complex) components enriched in the CENP-A chromatin of human cells. *Genes Cells* 11: 673–684

Joglekar AP, Bloom K, Salmon ED (2009) In vivo protein architecture of the eukaryotic kinetochore with nanometer scale accuracy. *Curr Biol* 19: 694–699

John S, Howe L, Tafrov ST, Grant PA, Sternglanz R, Workman JL (2000) The something about silencing protein, Sas3, is the catalytic subunit of NuA3, a yTAF(II)30-containing HAT complex that interacts with the Spt16 subunit of the yeast CP (Cdc68/Pob3)-FACT complex. *Genes Dev* 14: 1196–1208

Kato H, Jiang J, Zhou BR, Rozendaal M, Feng H, Ghirlando R, Xiao TS, Straight AF, Bai Y (2013) A conserved mechanism for centromeric nucleosome recognition by centromere protein CENP-C. *Science* 340: 1110–1113

Keith KC, Baker RE, Chen Y, Harris K, Stoler S, Fitzgerald-Hayes M (1999) Analysis of primary structural determinants that distinguish the centromere-specific function of histone variant Cse4p from histone H3. *Mol Cell Biol* 19: 6130–6139

Kitamura E, Tanaka K, Kitamura Y, Tanaka TU (2007) Kinetochore microtubule interaction during S phase in *Saccharomyces cerevisiae*. *Genes Dev* 21: 3319–3330

Kudalkar EM, Scarborough EA, Umbreit NT, Zelter A, Gestaut DR, Riffle M, Johnson RS, MacCoss MJ, Asbury CL, Davis TN (2015) Regulation of outer kinetochore Ndc80 complex-based microtubule attachments by the central kinetochore Mis12/MIND complex. *Proc Natl Acad Sci USA* 112: E5583–E5589

Kunitoku N, Sasayama T, Marumoto T, Zhang D, Honda S, Kobayashi O, Hatakeyama K, Ushio Y, Saya H, Hirota T (2003) CENP-A phosphorylation by Aurora-A in prophase is required for enrichment of Aurora-B at inner centromeres and for kinetochore function. *Dev Cell* 5: 853–864

Longtine MS, McKenzie A III, Demarini DJ, Shah NG, Wach A, Brachat A, Philippsen P, Pringle JR (1998) Additional modules for versatile and economical PCR-based gene deletion and modification in *Saccharomyces cerevisiae*. *Yeast* 14: 953–961

Lu R, Wang GG (2013) Tudor: a versatile family of histone methylation "readers". *Trends Biochem Sci* 38: 546–555

McNally FJ, Rine J (1991) A synthetic silencer mediates *SIR*-dependent functions in *Saccharomyces cerevisiae*. *Mol Cell Biol* 11: 5648–5659

Meluh PB, Yang P, Glowczewski L, Koshland D, Smith MM (1998) Cse4p is a component of the core centromere of *Saccharomyces cerevisiae*. *Cell* 94: 607–613

Musacchio A, Desai A (2017) A molecular view of kinetochore assembly and function. *Biology* 6: E5

Nikolovska-Coleska Z, Wang R, Fang X, Pan H, Tomita Y, Li P, Roller PP, Krajewski K, Saito NG, Stuckey JA, Wang S (2004) Development and optimization of a binding assay for the XIAP BIR3 domain using fluorescence polarization. *Anal Biochem* 332: 261–273

Nogales E, Ramey VH (2009) Structure-function insights into the yeast Dam1 kinetochore complex. *J Cell Sci* 122: 3831–3836

Okada M, Cheeseman IM, Hori T, Okawa K, McLeod IX, Yates JR III, Desai A, Fukagawa T (2006) The CENP-H-I complex is required for the efficient incorporation of newly synthesized CENP-A into centromeres. *Nat Cell Biol* 8: 446–457

Ortiz J, Stemmann O, Rank S, Lechner J (1999) A putative protein complex consisting of Ctf19, Mcm21, and Okp1 represents a missing link in the budding yeast kinetochore. *Genes Dev* 13: 1140–1155

Patel DJ, Wang Z (2013) Readout of epigenetic modifications. *Annu Rev Biochem* 82: 81–118

Poddar A, Roy N, Sinha P (1999) MCM21 and MCM22, two novel genes of the yeast *Saccharomyces cerevisiae* are required for chromosome transmission. *Mol Microbiol* 31: 349–360

Ranjitkar P, Press MO, Yi X, Baker R, MacCoss MJ, Biggins S (2010) An E3 ubiquitin ligase prevents ectopic localization of the centromeric histone H3 variant via the centromere targeting domain. *Mol Cell* 40: 455–464

Reifsnyder C, Lowell J, Clarke A, Pillus L (1996) Yeast silencing genes and human genes associated with AML and HIV-1 Tat interactions are homologous with acetyltransferases. *Nat Genet* 14: 42–49

Roth SY, Denu JM, Allis CD (2001) Histone acetyltransferases. *Annu Rev Biochem* 70: 81–120

Samel A, Cuomo A, Bonaldi T, Ehrenhofer-Murray AE (2012) Methylation of CenH3 arginine 37 regulates kinetochore integrity and chromosome segregation. *Proc Natl Acad Sci USA* 109: 9029–9034

Samel A, Nguyen TKL, Ehrenhofer-Murray AE (2017) Defects in methylation of arginine 37 on CENP-A/Cse4 are compensated by the ubiquitin ligase complex Ubr2/Mub1. *FEMS Yeast Res* 17: fox009

Sathyan KM, Fachinetti D, Foltz DR (2017) alpha-amino trimethylation of CENP-A by NRMT is required for full recruitment of the centromere. *Nat Commun* 8: 14678

Schmitzberger F, Harrison SC (2012) RWD domain: a recurring module in kinetochore architecture shown by a Ctf19-Mcm21 complex structure. *EMBO Rep* 13: 216–222

Schmitzberger F, Richter MM, Gordiyenko Y, Robinson CV, Dadlez M, Westermann S (2017) Molecular basis for inner kinetochore configuration through RWD domain-peptide interactions. *EMBO J* 36: 3458–3482

Sherman F (1991) Getting started with yeast. *Methods Enzymol* 194: 3–21

Shivaraju M, Unruh JR, Slaughter BD, Mattingly M, Berman J, Gerton JL (2012) Cell-cycle-coupled structural oscillation of centromeric nucleosomes in yeast. *Cell* 150: 304–316

Sikorski RS, Hieter P (1989) A system of shuttle vectors and yeast host strains designed for efficient manipulation of DNA in *Saccharomyces cerevisiae*. *Genetics* 122: 19–27

Stoler S, Keith KC, Curnick KE, Fitzgerald-Hayes M (1995) A mutation in CSE4, an essential gene encoding a novel chromatin-associated protein in yeast, causes chromosome nondisjunction and cell cycle arrest at mitosis. *Genes Dev* 9: 573–586

Studier FW (2005) Protein production by auto-induction in high density shaking cultures. *Protein Expr Purif* 41: 207–234

Tan S, Kern RC, Selleck W (2005) The pST44 polycistronic expression system for producing protein complexes in *Escherichia coli*. *Protein Expr Purif* 40: 385–395

Varma D, Salmon ED (2012) The KMN protein network–chief conductors of the kinetochore orchestra. *J Cell Sci* 125: 5927–5936

Waterborg JH (2000) Steady-state levels of histone acetylation in *Saccharomyces cerevisiae*. *J Biol Chem* 275: 13007–13011

Westermann S, Schleiffer A (2013) Family matters: structural and functional conservation of centromere-associated proteins from yeast to humans. *Trends Cell Biol* 23: 260–269

Wigge PA, Kilmartin JV (2001) The Ndc80p complex from *Saccharomyces cerevisiae* contains conserved centromere components and has a function in chromosome segregation. *J Cell Biol* 152: 349–360

Wisniewski J, Hajj B, Chen J, Mizuguchi G, Xiao H, Wei D, Dahan M, Wu C (2014) Imaging the fate of histone Cse4 reveals *de novo* replacement in S phase and subsequent stable residence at centromeres. *Elife* 3: e02203

Wittschieben BO, Otero G, de Bizemont T, Fellows J, Erdjument-Bromage H, Ohba R, Li Y, Allis CD, Tempst P, Svejstrup JQ (1999) A novel histone acetyltransferase is an integral subunit of elongating RNA polymerase II holoenzyme. *Mol Cell* 4: 123–128

Xiao H, Wang F, Wisniewski J, Shaytan AK, Ghirlando R, FitzGerald PC, Huang Y, Wei D, Li S, Landsman D, Panchenko AR, Wu C (2017) Molecular basis of CENP-C association with the CENP-A nucleosome at yeast centromeres. *Genes Dev* 31: 1958–1972

Zeitlin SG, Shelby RD, Sullivan KF (2001) CENP-A is phosphorylated by Aurora B kinase and plays an unexpected role in completion of cytokinesis. *J Cell Biol* 155: 1147–1157